Japanese Journal of Applied Physics **55**, 067302 (2016)
http://doi.org/10.7567/JJAP.55.067302

REGULAR PAPER

Effect of holed reflector on acoustic radiation force in noncontact ultrasonic dispensing of small droplets

Hiroki Tanaka[1]*, Yuji Wada[2], Yosuke Mizuno[1], and Kentaro Nakamura[1]

[1]*Precision and Intelligence Laboratory, Tokyo Institute of Technology, Yokohama 226-8503, Japan*
[2]*Faculty of Science and Technology, Seikei University, Musashino, Tokyo 180-8633, Japan*

*E-mail: htanaka@sonic.pi.titech.ac.jp

Received October 8, 2015; accepted April 11, 2016; published online May 31, 2016

We investigated the fundamental aspects of droplet dispensing, which is an important procedure in the noncontact ultrasonic manipulation of droplets in air. A holed reflector was used to dispense a droplet from a 27.4 kHz standing-wave acoustic field to a well. First, the relationship between the hole diameter of the reflector and the acoustic radiation force acting on a levitated droplet was clarified by calculating the acoustic impedance of the point just above the hole. When the hole diameter was half of (or equal to) the acoustic wavelength λ, the acoustic radiation force was ~80% (or 50%) of that without a hole. The maximal diameters of droplets levitated above the holes through flat and half-cylindrical reflectors were then experimentally investigated. For instance, with the half-cylindrical reflector, the maximal diameter was 5.0 mm for a hole diameter of 6.0 mm, and droplets were levitatable up to a hole diameter of 12 mm (~λ).

1. Introduction

The noncontact transport of small components, powders, and droplets is an increasingly important technology in the pharmaceutical industry as well as in new material science and engineering. To date, various methods, such as those using air pressure[1)] and magnetic/electric fields,[2,3)] have been studied. Compared with these methods, ultrasonic levitation, which is based on the phenomenon of objects much smaller than the wavelength of an acoustic standing wave being trapped at the nodal points of the pressure field, has several important advantages, such as tranquility, cost efficiency, and applicability to nonelectric/magnetic objects, and thus, it has attracted considerable attention.[4–11)] In the meantime, the ultrasonic manipulation of small particles or cells in liquid has been extensively studied by many research groups.[12–14)]

Our research goal is to implement all the procedures of noncontact transport of objects (especially droplets) in air based on ultrasonics, to wit, injection, linear transport, direction switching, mixing, ejection, analysis, and dispensing, as shown in Fig. 1. We can utilize a variety of ultrasonic technologies to handle small objects in air.[15–23)] Although linear transport,[24–26)] direction switching,[27)] mixing,[28)] and ejection[29)] have already been demonstrated, the other procedures need to be studied to accomplish the goal.

We here focus on one of the important procedures of the manipulation, i.e., droplet dispensing, the concept of which is schematically shown in Fig. 2. A vibrating plate and a reflector with some holes through it are employed to generate an ultrasonic standing wave between them, and multiple droplets are trapped at the nodal points. Then, by turning off or lowering the vibration, the droplets are dispensed into a microplate through the holes on the reflector. To realize this concept, before performing the simultaneous dispensing of multiple droplets, certain fundamental aspects, including the acoustic radiation force acting on an object levitated above a single hole as well as the maximal diameter of a droplet that can be levitated, require clarification.

In this paper, we report results the of numerical simulations of the relationship between the hole diameter of a reflector and the acoustic radiation force acting on a levitated droplet, as well as of an experimental investigation of the maximal

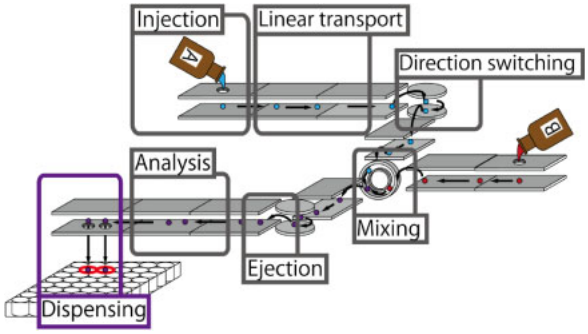

Fig. 1. (Color online) Future vision of noncontact ultrasonic transport of droplets.

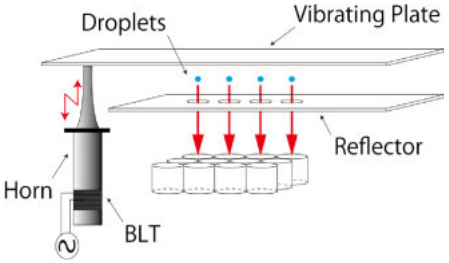

Fig. 2. (Color online) Conceptual setup of multiple-droplet dispensing system. BLT: bolt-clamped Langevin-type transducer.

diameters of droplets that can be levitated above holes on reflectors with two different shapes. First, by applying a finite-element method (FEM) to a model comprising a flat reflector and a transducer, we calculate the acoustic impedance of the point just above a hole, based on which the reflectivity of the holed reflector is plotted as a function of hole diameter. The trend of the acoustic radiation force acting on a levitated object with respect to the hole diameter is then investigated. Subsequently, to verify whether the FEM results hold true even when the disturbance of the acoustic field by a levitated object is considered, we experimentally investigate the minimal vibration velocity of a transducer required to levitate a polystyrene sphere and the maximal diameter of a droplet levitated just above a hole. Here, we utilize not only

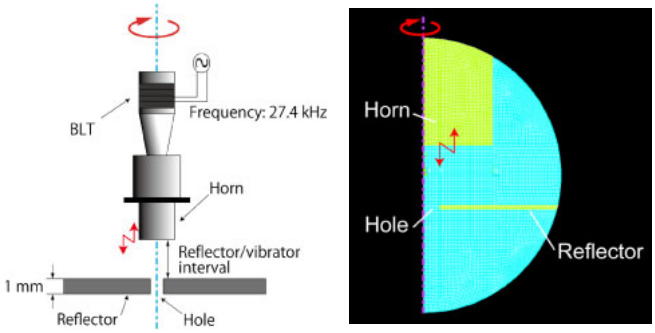

Fig. 3. (Color online) Axis-symmetric models used in (a) experiments and (b) simulation.

a flat reflector but also a half-cylindrical reflector, with which higher-pressure standing waves can be excited.[26] The obtained simulation and experimental results are compared and discussed.

2. Simulation

To generate acoustic standing waves, the reflectivity of the reflector needs to be sufficiently high. We therefore need to investigate the effect of a hole on the reflector. Here, using an FEM (ANSYS Mechanical APDL 14.5), we calculated the acoustic impedance of the point just above a hole on a flat reflector to investigate the relationship between the hole diameter and the acoustic radiation force acting on a levitated droplet. An axis-symmetrical model containing a flat reflector with a hole and a vibrator was employed, as shown in Figs. 3(a) and 3(b). (Note that, owing to a high computational cost, it is practically difficult to employ a non-axis-symmetrical model if a middle-class personal computer is used.) We assumed a horn of 30.0 mm diameter to be vibrating at 27.4 kHz with a maximal zero-to-peak velocity of 0.75 m/s, the sound speed in air (c) to be 340 m/s, and the air density (ρ) to be 1.2 kg/m^3. The physical parameters, with the exception of the hole diameter of the reflector, are treated as constants because the acoustic impedance is affected by the other parameters, such as the vibrator-reflector interval. The square mesh size for calculation was set to 0.5 mm. The acoustic impedance at each element just above the hole, which is expressed as the acoustic pressure divided by the particle velocity of air in the vertical direction,[30] was calculated as a function of hole diameter. The dependence of the acoustic impedance above the hole, Z_h, on the hole diameter was then calculated by taking an area-based weighted average using the following equation:

$$Z_h = \sum_{n=1}^{N} \frac{L^2(2n-1)}{r_h^2} Z_n, \tag{1}$$

where L is the square mesh size, r_h is the hole radius (unit: mm), Z_n is the acoustic impedance of the n-th mesh from the symmetric axis ($n = 1, 2, \ldots, N$, where $N = r_h/L$).

Figure 4(a) shows the result, in which the horizontal axis is the product of the wavenumber k and the hole diameter d, and the vertical axis is Z_h divided by the specific acoustic impedance of air in free space, $\rho c = 408\,\mathrm{kg/m^2}$, so that the values on both axes become nondimensional. With increasing kd, the real part of Z_h exceeded its imaginary part at $kd \sim 2$, and then converged to 1, which is similar to that observed for the radiation impedance with a hole.[31] When kd is lower than 1, the imaginary part of the acoustic impedance is dominant, resulting in the total reflection of the acoustic waves. This indicates that the generated standing waves stably levitate a droplet. The thickness of the reflector, i.e., the length of the hole, generally plays a major role in determining the difference between the acoustic impedance at the outlet of the hole and that at the inlet. In this model, the length of the hole (1.0 mm) corresponds to approximately $0.1 \times \lambda$, and has almost no effect on the impedance.

Next, assuming that planar waves are radiated from the end of the horn, we calculated the reflectivity of the holed reflector within the diameter range of the horn. For this purpose, we defined Z_r as the absolute value of the acoustic impedance of the point just above the reflector (by more than 0.5 mm), which is averaged over the diameter range of less than 30.0 mm. We then plotted Z_r as a function of kd, as shown in Fig. 4(b). Here, Z_r was calculated as

$$Z_r = \sum_{n=1}^{M} \frac{L^2(2n-1)}{r_t^2} |Z_n|, \tag{2}$$

where r_t is the horn radius (unit: mm) and $|Z_n|$ is the absolute value of the acoustic impedance of the n-th mesh from the symmetric axis ($n = 1, 2, \ldots, M$, where $M = r_t/L$). The

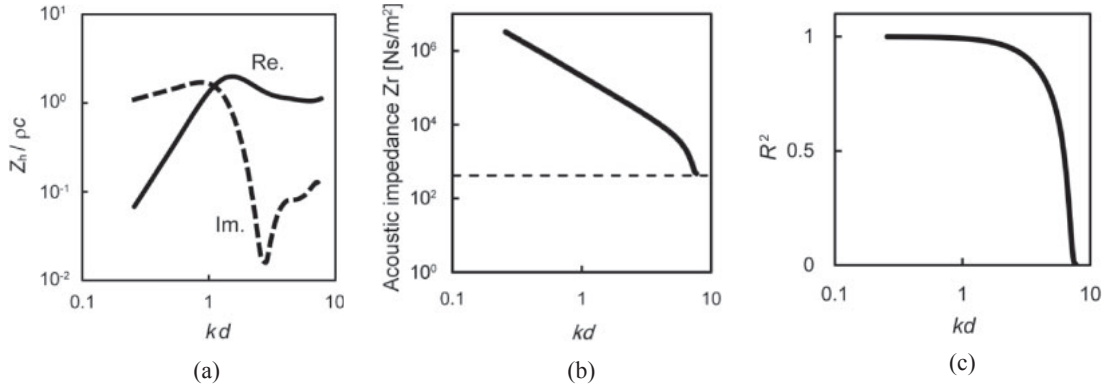

Fig. 4. (a) Acoustic impedance of the point 0–0.5 mm above the hole, Z_h, divided by the specific acoustic impedance of air (ρc) vs product of the wavenumber k and hole diameter d. The solid and dashed lines indicate real and imaginary parts, respectively. (b) Absolute value of the acoustic impedance of the point 0.5 mm above the hole (within the diameter range of less than 30.0 mm), Z_r, vs kd. The dashed line indicates the ρc value. (c) Square of the reflectivity R vs kd.

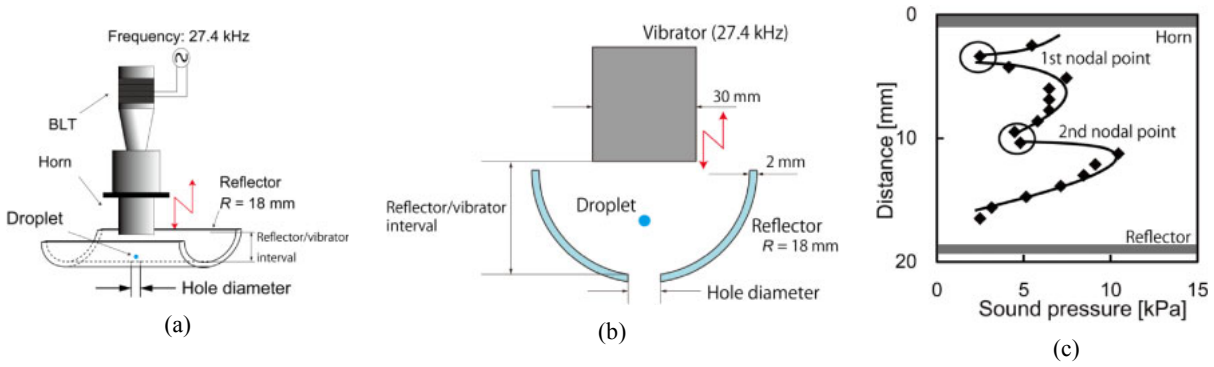

Fig. 5. (Color online) (a) Experimental setup for dispensing a single droplet, (b) its cross-sectional view, and (c) measured sound pressure above the hole vs distance from the BLT horn.

specific acoustic impedance of air (ρc), indicated by a dashed line, was equal to Z_r when $kd = 8$. This result indicates that a standing wave cannot be excited when the diameter of the holed reflector is larger than $1.3 \times \lambda$. When the hole diameter approached zero, the acoustic impedance converged to the specific acoustic impedance of aluminum, which is the material used for the reflector. The square of the reflectivity, $R = (Z_r - \rho c)/(Z_r + \rho c)$, was then plotted as a function of kd using ρc [Fig. 4(c)]. This result agrees with the trend of the relationship between kd and the acoustic radiation force F_r acting on a levitated object because F_r correlates with R.[2,32,33] With increasing kd, the levitation force decreased. For example, when the hole diameter was half the wavelength ($kd = 3$), the acoustic radiation force was approximately 80% of that without a hole, while when the hole diameter was identical to the wavelength ($kd = 6$), the radiation force was 50% of that without a hole. This result indicates that when the hole diameter is sufficiently small compared with the wavelength, the generated acoustic field is a standing wave, while when the hole diameter becomes larger, the field contains a considerable traveling-wave component, resulting in a reduced levitation force.

3. Experiments

Subsequently, we performed an experiment using two types of reflectors, i.e., flat and half-cylindrical reflectors. The setup of the former is shown in Fig. 3(a), while the setup and cross-sectional view of the latter are depicted in Figs. 5(a) and 5(b), respectively. A bolt-clamped Langevin transducer (BLT), with a step horn with a step-up ratio of 1.8 and a radiation surface diameter of 30.0 mm, was driven at 27.4 kHz. An acrylic half-cylindrical plate of 18 mm radius, through which a hole was drilled, was employed as a reflector.[26] Ethanol was used as a droplet, which was manually injected above the hole with a syringe.

To experimentally determine which of the two nodal points should be used to levitate a droplet in the dispensing system, using the half-cylindrical reflector, we measured the acoustic pressure distribution along the vertical axis through the hole using a 1/8-in. microphone (ACO 7118), when the horn end was vibrating at a zero-to-peak velocity of 1.25 m/s, as shown in Fig. 5(c). As this measurement was performed to determine the position of the levitated object, the disturbance of the acoustic field by the microphone was neglected. The hole diameter was 7.0 mm. As was expected, two nodal points were observed. The lower nodal point at $D = 10$ mm was selected as the position where the droplet would be levitated, because the antinode at $D = 12$ mm was higher in sound pressure, leading to a larger acoustic radiation force and thus a more stable levitation.

To verify the simulation result [Fig. 4(c)], we then experimentally investigated the minimal vibration velocity of the transducer required for levitation and the relationship between the hole diameter and the transducer-reflector interval. The zero-to-peak vibration velocity was calculated from the driving current using the force factor, equal to 0.59 N/V for this transducer, as measured before the experiment. Rather than ethanol, a polystyrene sphere of 2.5 mm diameter was employed in this experiment for the following reasons: (1) it is not nebulized, (2) it has constant volume, mass, and surface area, and (3) it is sufficiently light to measure slight changes in acoustic field. Using both types of reflectors, the hole diameter was varied from 0 to 12.0 mm in steps of 2.0 mm. The transducer-reflector interval was set to three different values with a step of 0.5 mm, for which the polystyrene sphere was levitated right above the hole with any diameter. Note that objects occasionally avoid being levitated above a hole.[23]

Figures 6(a) and 6(b) show the minimal vibration velocity of the transducer plotted as a function of kd for the flat and half-cylindrical reflectors, respectively. Points for which the hole diameter was 0 mm were plotted as $kd = 0.1$. Generally, the required velocity for the half-cylindrical reflector was lower than that for the flat one, which is valid considering the results in Ref. 26. As the hole diameter increased, the minimal vibration velocity required to keep the object levitated also increased. Particularly for the flat reflector, when the hole diameter was larger than half the wavelength ($kd = 3$), the required velocity was higher than that for smaller holes. Regardless of reflector shape, a higher vibration velocity was required when $kd = 1$ than that when $kd = 2$, which suggests that some resonance is induced at $kd \sim 1$; a more detailed study regarding this point is needed. As expected from the simulation of acoustic impedance and reflectivity, in order to compensate for the leakage of sound energy from the hole and maintain the sound intensity, high-amplitude vibration is required.

Finally, using the flat and half-cylindrical reflectors, we experimentally investigated the relationship between kd and the maximal diameter of a droplet levitated above a hole, as

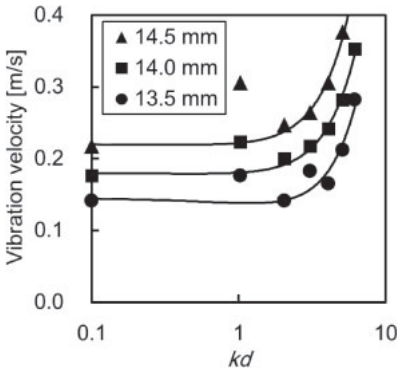

(a)

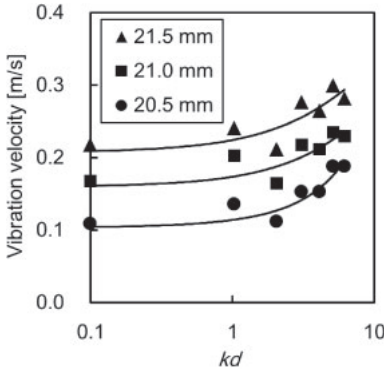

(b)

Fig. 6. (a) Minimum driving current applied to the BLT vs product of the wavenumber k and hole diameter d with the (a) flat and (b) half-cylindrical reflectors. The solid curves indicate the trends.

shown in Fig. 7. Again, points for which the hole diameter was 0 mm were plotted as $kd = 0.1$. The droplet was introduced to the lower nodal point with a syringe. A photograph of the levitated droplet was taken along a horizontal axis using a high-speed camera, and its diameter was measured. Here, as the droplet was not a complete sphere, for the direct comparison with the hole diameter, we defined the "diameter" of the droplet as its diameter in the horizontal plane. We define the "maximal diameter" of the levitated droplet as the largest diameter that does not exceed the limit at which the droplet becomes nebulized or falls off the nodal point. The driving current of the transducer and the transducer-reflector interval were each adjusted according to the hole diameter. Generally, larger droplets were levitated for the half-cylindrical reflector than for the flat one. When the reflector was flat, the vibration velocity required to levitate the object markedly increased when the hole diameter exceeded ~70% of the wavelength. For example, the maximal diameter of a levitatable droplet was 2.5 mm for a hole diameter of 6.0 mm (approximately half the wavelength). However, when the hole diameter was larger than 8 mm (~70% of the wavelength), droplets were not levitated. These trends are in good agreement with the simulation result shown in Fig. 4(c). When the half-cylindrical reflector was used, the required vibration velocity increased gradually, regardless of the hole diameter. The maximal diameter of a levitatable droplet was, for instance, 5.0 mm for a hole diameter of 6.0 mm; a droplet was levitatable when the hole diameter was up to 12 mm, which is close to the wavelength.

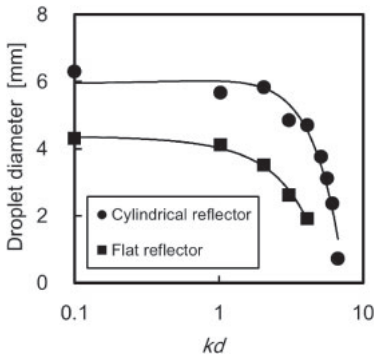

Fig. 7. Maximal diameter of the levitatable droplet vs product of the wavenumber k and hole diameter d with the flat and half-cylindrical reflectors. The solid curves indicate the trends.

4. Conclusions

The basic aspects of one of the most important procedures of noncontact ultrasonic manipulation of droplets in air — droplet dispensing — were investigated. First, using an FEM, we numerically analyzed the relationship between the hole diameter of a reflector and the acoustic radiation force acting on a levitated droplet. In this simulation, we calculated the acoustic impedance at the point just above a hole and the reflectivity of the holed reflector, and investigated the relationship between the applied acoustic radiation force and the hole diameter. As a result, it was found that when the hole diameter was half of (or equal to) the acoustic wavelength, the acoustic radiation force was ~80% (or 50%) of that in the absence of a hole. Subsequently, the maximal diameters of droplets levitated above holes through flat and half-cylindrical reflectors were experimentally investigated. With the flat reflector, the maximal diameter was 2.5 mm for a hole diameter of 6.0 mm (approximately half the wavelength); when the hole diameter was larger than 8 mm (approximately 70% of the wavelength), no droplet was levitated. In contrast, with the half-cylindrical reflector, the maximal diameter was 5.0 mm for a hole diameter of 6.0 mm, and a droplet was levitatable up to the hole diameter of 12 mm, which is close to the wavelength. We believe that these results will be useful in the development of noncontact ultrasonic droplet dispensers, providing significant information for the demonstration of the simultaneous dispensing of multiple droplets and thus for the realization of noncontact ultrasonic transport systems in the future.

Acknowledgment

This work was partially supported by JSPS KAKENHI Grant Number 26289054.

1) S. Konishi, M. Harada, Y. Ogami, Y. Daiho, Y. Mita, and H. Fujita, ETFA 6th Int. Conf., 1997, p. 232.
2) S. Mukhopadhyay, J. Donaldson, G. Sengupta, S. Yamada, C. Chakraborty, and D. Kacprzak, IEEE Trans. Magn. **39**, 3220 (2003).
3) F. Hellman, E. M. Gyorgy, D. W. Johnson, H. M. O'Bryan, and R. C. Sherwood, J. Appl. Phys. **63**, 447 (1988).
4) R. R. Whymark, Ultrasonics **13**, 251 (1975).
5) E. G. Lierke, Acustica **82**, 220 (1996).
6) H. Hatano, Y. Kanai, Y. Ikegami, T. Fujii, and K. Sato, Nippon Onkyo Gakkaishi **47**, 40 (1991) [in Japanese].
7) E. Benes, M. Groschl, H. Nowotny, F. Trampler, T. K. Keijzer, H. Bohm, S.

Radel, L. Gherardini, J. J. Hawkes, R. Konig, and Ch. Delouvroy, Proc. IEEE Ultrasonics Symp., 2001, p. 649.
8) Y. Hashimoto, Y. Koike, and S. Ueha, J. Acoust. Soc. Am. **103**, 3230 (1998).
9) Y. Hashimoto, Y. Koike, and S. Ueha, J. Acoust. Soc. Am. **100**, 2057 (1996).
10) R. Yano, M. Aoyagi, H. Tamura, and T. Takano, Jpn. J. Appl. Phys. **50**, 07HE29 (2011).
11) Y. Yamayoshi and S. Hirose, Jpn. J. Appl. Phys. **50**, 07HE28 (2011).
12) T. Kozuka, K. Yasui, S. Hatanaka, T. Tuziuti, K. Suzuki, and A. Towata, Jpn. J. Appl. Phys. **50**, 07HE27 (2011).
13) K. Masuda, R. Nakamoto, N. Watarai, R. Koda, Y. Taguchi, T. Kozuka, Y. Miyamoto, T. Kakimoto, S. Enosawa, and T. Chiba, Jpn. J. Appl. Phys. **50**, 07HF11 (2011).
14) M. Takeuchi and K. Yamanouchi, Jpn. J. Appl. Phys. **33**, 3045 (1994).
15) A. Haake and J. Dual, Ultrasonics **42**, 75 (2004).
16) T. Kozuka, K. Yasui, T. Tuziuti, A. Towada, and Y. Iida, Jpn. J. Appl. Phys. **46**, 4948 (2007).
17) T. Kozuka, K. Yasui, T. Tuziuti, A. Towada, and Y. Iida, Jpn. J. Appl. Phys. **47**, 4336 (2008).
18) J. Hawkes, J. Cefai, D. Barrow, W. Coakley, and L. Briarty, J. Phys. D **31**, 1673 (1998).
19) W. Coakley, J. Hawkes, M. Sobanski, C. Cousins, and J. Spengler, Ultrasonics **38**, 638 (2000).
20) A. Haake and J. Dual, J. Acoust. Soc. Am. **117**, 2752 (2005).
21) A. Osumi, K. Doi, and Y. Ito, Jpn. J. Appl. Phys. **50**, 07HE30 (2011).
22) K. Matsumoto and H. Miura, Jpn. J. Appl. Phys. **51**, 07GE05 (2012).
23) H. Tanaka, Y. Wada, Y. Mizuno, and K. Nakamura, Jpn. J. Appl. Phys. **52**, 100201 (2013).
24) D. Koyama and K. Nakamura, IEEE Trans. Ultrason. Ferroelectr. Freq. Control **57**, 1152 (2010).
25) Y. Ito, D. Koyama, and K. Nakamura, Acoust. Sci. Technol. **31**, 420 (2010).
26) M. Ding, D. Koyama, and K. Nakamura, Appl. Phys. Express **5**, 097301 (2012).
27) D. Koyama and K. Nakamura, IEEE Trans. Ultrason. Ferroelectr. Freq. Control **57**, 1434 (2010).
28) S. Murakami, D. Koyama, and K. Nakamura, AIP Conf. Proc. **1433**, 783 (2011).
29) R. Nakamura, Y. Mizuno, and K. Nakamura, Jpn. J. Appl. Phys. **52**, 07HE02 (2013).
30) J. R. Frederick, *Ultrasonic Engineering* (Wiley, New York, 1965) p. 27.
31) S. Nishiyama, K. Ikegaya, Z. Yamaguchi, and M. Okujima, *Onkyo Shindo Kogaku* (Acoustic and Vibration Engineering) (Corona, Tokyo, 1979) p. 67 [in Japanese].
32) L. P. Gor'kov, Sov. Phys. Dokl. **6**, 773 (1962).
33) T. Kamakura, *Hisenkei Onkyo: Kiso to Oyo* (Nonlinear Acoustics: Fundamentals and Applications) (Corona, Tokyo, 2014) [in Japanese].